

1

ORIGINAL SUBMISSION

2

3

Simulating Contact Using the Elastic Foundation Algorithm in

4

OpenSim

¹Michael W. Hast, Ph.D., ¹Brett G. Hanson, ²Josh R. Baxter, Ph.D.

Study conducted at The University of Pennsylvania, Philadelphia, Pennsylvania, U.S.A.

¹*Biedermann Lab for Orthopaedic Research, Department of Orthopaedic Surgery, The University of Pennsylvania, Philadelphia, PA 19104 U.S.A.*

²*Human Motion Lab, Department of Orthopaedic Surgery, The University of Pennsylvania, Philadelphia, PA 19104 U.S.A.*

5

6

7

*Address correspondence and reprint requests to Michael Hast, Biedermann Lab for Orthopaedic Research, 3737 Market Street, 10th Floor Suite 1050, The University of Pennsylvania, Philadelphia, PA 19104 U.S.A.

9

[e-mail: hast@penncmedicine.upenn.edu phone: 215-898-7380]

10

11 **WORD COUNT (Abstract):** 234

12 **WORD COUNT (Introduction – Discussion):** 1,649

13 **SUBMISSION TYPE:** Short Communication

14 **KEY WORDS:** computational simulation, contact forces, tibiofemoral forces,

15

16

17 **Abstract**

18 Modeling joint contact is necessary to test many questions using simulation paradigms,
19 but this portion of OpenSim is not well understood. The purpose of this study was to
20 provide a guide for implementing a validated elastic foundation contact model in
21 OpenSim. First, the load-displacement properties of a stainless steel ball bearing and ultra
22 high molecular weight polyethylene (UHMWPE) slab were recorded during a controlled
23 physical experiment. These geometries were imported and into OpenSim and contact
24 mechanics were modeled with the on-board elastic foundation algorithm. Particle swarm
25 optimization was performed to determine the elastic foundation model stiffness
26 ($2.14 \times 10^{11} \pm 6.81 \times 10^9$ N/m) and dissipation constants (0.999 ± 0.003). Estimations of
27 contact forces compared favorably with blinded experimental data (root mean square
28 error: 87.58 ± 1.57 N). Last, total knee replacement geometry was used to perform a
29 sensitivity analysis of material stiffness and mesh density with regard to penetration
30 depth and computational time. These simulations demonstrated that material stiffnesses
31 between 10^{11} and 10^{12} N/m resulted in realistic penetrations (< 0.15 mm) when subjected
32 to 981N loads. Material stiffnesses between 10^{13} and 10^{15} N/m increased computation
33 time by factors of 12-23. This study shows the utility of performing a simple physical
34 experiment to tune model parameters when physical components of orthopaedic implants
35 are not available to the researcher. It also demonstrates the efficacy of employing the on-
36 board elastic foundation algorithm to create realistic simulations of contact between
37 orthopaedic implants.

38

39

40 **Title**

41 Simulating Contact Using the Elastic Foundation Algorithm in OpenSim

42 **Introduction**

43 Predicting articular joint function and loading continues to be an important
44 research topic in orthopaedics. Effective clinical treatment and design of orthopaedic
45 implants requires a thorough understanding of joint loads throughout dynamic activities
46 of daily living. Computer simulation has become a widely used method for the
47 determination of joint contact forces during dynamic tasks, as it is not subject to the same
48 constraints that accompany physical experimental investigations. Modeling joint contact
49 using an elastic foundation (EF) paradigm is a commonly utilized approach because of its
50 cheap computational cost, a desirable characteristic for integrating joint contact into
51 muscle-driven simulations (Kim et al., 2009; Lenhart et al., 2015; Lin and Fregly, 2010;
52 Schmitz and Piovesan, 2016; Shelburne et al., 2006; Taylor et al., 2004).

53 OpenSim (Delp et al., 2007) is a widely used and freely available musculoskeletal
54 modeling software package that has an onboard EF contact algorithm. Based on the
55 history of forum posts and a dearth of publications using this paradigm, this Opensim
56 feature is not well understood by many users (Dunne et al., 2013, 2017a, 2017b). Perhaps
57 for this reason, the on-board algorithm is seldom used for the purposes of estimating joint
58 forces. Although the mathematical concept behind the EF algorithm is outlined in several
59 publications (Sherman et al., 2011; Uchida et al., 2015), details regarding validation and
60 day-to-day use remain confusing for end users. For example, the material stiffness
61 constant is described with the following equation:

$$\text{Stiffness Constant} = \frac{\text{Young's Modulus}}{\text{Material Thickness}}$$

62 It is unclear if other variables within the model (dissipation, mesh density, geometric
63 complexity) affect accuracy and computation time, two important metrics of performance
64 in computational modeling.

65 The purpose of the present work was to provide end users with a better
66 understanding of the on-board EF algorithm in OpenSim, so that estimations of joint
67 contact forces can be made readily, with accuracy, and with consistency. To do this, we
68 developed a simple experiment and concomitant OpenSim models that provide guidelines
69 for determining EF input parameters. For simplicity, a validation experiment was first
70 performed to investigate the estimation of contact forces between a sphere and a plate.
71 To demonstrate a more complex and biomechanically relevant simulation, contact of a
72 total knee arthroplasty (TKA) was simulated to test the sensitivity of simulation
73 performance to small changes to model parameters.

74

75 **Methods**

76 *Tuning and Testing Contact Parameters: Sphere-on-Plate*

77 Elastic foundation parameters for simple model were established using a physical
78 experiment. A tightly toleranced 5.08 cm diameter 316L stainless steel ball bearing and a
79 15.24 x 7.62 x 0.95 cm thick slab of ultra high molecular weight polyethylene
80 (UHMWPE) underwent mechanical testing. The UHMWPE rested freely on the bed of
81 the test frame (Electroforce 3330, TA Instruments, New Castle, DE) and the sphere was
82 placed on the slab, directly under the actuator (Figure 1A). To simulate dynamic loading,
83 the actuator imparted loads between 0 – 750 N at 1 Hz for 50 cycles while force-

84 displacement data were collected at 100 Hz. This protocol was repeated 10 times, taking
85 care to use unblemished areas of the deformable plastic for each trial.

86 Computer generated three dimensional (3D) renderings of the sphere and plate
87 (Solidworks 2017, Dassault Systèmes, Waltham, MA) were imported into OpenSim
88 (version 3.3, Appendix A) and defined as an EF contact model. Prior to being imported
89 into OpenSim, both 3D bodies were converted into watertight stereolithography (STL)
90 files in American Standard Code for Information Exchange (ASCII) format. Because EF
91 models predict forces based upon intersections of triangular faces of the 3D bodies, the
92 geometries were resampled to ensure the results from this study could be transferred to
93 more complex geometries. Specifically, the sphere was made up of 5852 faces and
94 oriented such that the pole was in contact with the plate. Rather than representing the
95 rectangular plate with 12 triangular faces, the mesh geometry was subdivided using open-
96 source mesh editing software (Meshlab, (Cignoni et al., 2008)) to have 30208 faces
97 (Figure 1B).

98 Stiffness and dissipation constants in the EF model were tuned by using an
99 optimization approach in the following manner. Based on pilot testing, the first 30
100 loading cycles of each 50 cycle trial exhibited substantial hysteresis. These cycles were
101 omitted to allow for preconditioning the UHMWPE slab. The force displacement
102 profiles of the 31st-40th trials were used to tune the computational model by simulating
103 prescribed motions in OpenSim that exactly replicated the displacements measured
104 during the physical experiment. Contact forces between the two bodies were calculated
105 in OpenSim with the onboard Force Reporter algorithm. The root mean square error
106 (RMSE) of the force versus time curve for the physical experiment and simulation was

107 used as an objective function. For each experimental trial, the values of stiffness and
108 dissipation were optimized using a hybrid “particleswarm/fmincon” function (MATLAB,
109 The Mathworks, Natick, MA) until the RMSE was minimized. Parameter values from all
110 trials were averaged to create optimized constants for stiffness and dissipation. Finally,
111 using the averaged constants, the displacements of the 40th-49th cycles of the
112 experimental trials were simulated and the resulting contact forces were estimated. The
113 50th cycle was omitted because completion of the last cycle in physical experiment was
114 not consistent across trials. To assess tuning accuracy, the newly estimated force versus
115 time curves were compared to their measured counterparts by calculating the RMSE of
116 the two curves.

117

118 *Simulating contact mechanics of total knee arthroplasty*

119 Tibiofemoral contact was modeled using a forward dynamic simulation to quantify
120 the relationships between computation time, implant penetration, material stiffness, and mesh
121 density. Computer aided designs of a cruciate-retaining total knee replacement (eTibia
122 (Fregly et al., 2012)) were imported into OpenSim and contact was modeled as an elastic
123 foundation element. ‘Drop and settle’ simulations (Figure 1C) were performed over a
124 series of model configurations to test the effects of tibial insert stiffness (10^9 to 10^{15} N/m)
125 mesh coarseness (100, 500, 1,000, 2,500, and 5,000 faces), and computational time.
126 Different amounts of weight bearing were also simulated by changing the mass of the
127 femoral component (1, 10, and 100kg). Center of mass position was adjusted to eliminate
128 rotation of the femoral component during simulations. Component penetration was
129 calculated as the vertical change in position of the femoral component center of mass
130 from the point of initial component contact to the final settling position. In total, 105

131 simulations were performed on a personal computer (Intel Core i5-6500, 3.20GHz, 8GB
132 RAM).

133 **Results and Discussion**

134 Stiffness and dissipation constants accurately predicted experimental cyclic
135 loading mechanics (Figure 2). The tuning optimization yielded average stiffness and
136 dissipation constants of $2.14 \times 10^{11} \pm 6.81 \times 10^9$ and 0.999 ± 0.003 , respectively. The
137 average stiffness constant found in the current study falls just outside of the range of
138 stiffness constants that are determined when dividing the modulus of UHMWPE (780 –
139 990 MPa (Kurtz, 2004)) by the thickness of 0.95 cm (8.2×10^{10} - 1.0×10^{11} N/m).

140 When comparing the experimental force versus time curves to the simulated ones,
141 the average root mean squared error (RMSE) was 87.58 ± 1.57 N. Because some
142 differences were due to a slight phase lag in the simulations, the estimated and measured
143 peak loads for all trials were also compared with a RMSE technique. In this case, the
144 average RMSE value was 32.45 ± 23.54 N. A table of results from all trials can be found
145 in Appendix B.

146 Simulated tibiofemoral penetration was below the *a priori* threshold of 0.15 mm
147 (Muratoglu et al., 2003) with the stiffness set at 10^{11} and 10^{12} N/m and the contact mesh
148 having at least 1000 faces (Figure 3). Lower stiffness values (10^9 and 10^{10} N/m) and
149 higher stiffness values (10^{13} to 10^{15} N/m) resulted in non-physiologic penetrations of
150 greater than 0.5 mm and component chattering, respectively. Computation time increased
151 as a function of both material stiffness and mesh density; however, overly stiff (10^{14} - 10^{15}
152 N/m) increased by a factor of 12 – 23 times longer than simulations with 10^{11} N/m.

153 Contact mechanics can be easily simulated using an EF paradigm when the
154 appropriate model parameters are selected. Component penetration is dependent on the
155 stiffness coefficient, where increased stiffness drastically increases computation time and
156 creates chattering behaviors between the contacting bodies, which is an artifact of
157 increased joint reaction loads (Appendix C). Mesh size also plays an important role in
158 overall simulation performance. Course meshes resulted in increased component
159 penetration and fine meshes increased computation time unnecessarily.

160 This experiment has several limitations. In the sphere on plate model, the
161 maximum load of 750 N was chosen because it represents approximately one body
162 weight of a 50th percentile male; however, the small contact patch between the plate and
163 sphere resulted in slightly higher maximum contact pressures (24.97 ± 4.04 MPa
164 Appendix D) than reported in TKA (~19 MPa) (Kwon et al., 2014). Although the current
165 experiment represents a worst-case scenario, future experiments may consider utilizing
166 more conforming geometries to better represent realistic stresses. The parameters of
167 static, dynamic, and viscous friction were all assumed to be negligible and therefore were
168 set to zero (Hast and Piazza, 2013; Thompson et al., 2011). This may not be the case for
169 more complex motions, and the parameters could readily be added to the optimization
170 routine. Finally, the TKA experiment was not validated with physical experiments. Such
171 an effort would require physical TKA implants and matching CAD geometries, which
172 were not available for this experiment.

173 **Conclusions**

174 OpenSim provides an EF algorithm that is freely available, computationally light,

175 and potentially powerful, but the tool is vastly underutilized because it is poorly
176 understood. This experiment represents the first published work that has outlined a
177 rigorous experimental approach to determine constants that will accurately predict forces
178 using the OpenSim EF contact algorithm. For the purposes of simplicity and practicality,
179 a simple stainless steel sphere and UHMWPE plate were used in the physical experiment,
180 which translated favorably into a virtual model of a TKA. When considering other
181 materials or other joints of the body, the same overall approach can be straightforwardly
182 adapted to make reasonable estimations joint contact forces.

183 **Acknowledgment**

184 The authors would like to thank the Biedermann family, who provided funding for this
185 study.

186 **Conflict of Interest Statement**

187 Michael Hast has sponsored research agreements with DePuy Synthes, Zimmer Biomet,
188 and Integra LifeSciences. None of these are relevant to the submission.

189 Brett Hanson has no conflicts to disclose.

190 Josh Baxter has no conflicts to disclose.

191

192 **Figure Legends**

193 **Figure 1** (A) A photograph showing the experimental setup involving a stainless
194 steel sphere in contact with a UHMWPE plate. The actuator of the test
195 frame imposed cyclic loads of 750N upon the sphere. (B) A screenshot

196 from the computational model of the physical experiment. The measured
197 displacements of the sphere during the physical experiment were
198 replicated, so that the stiffness and dissipation constants could be tuned.
199 (C) “Drop and settle” simulations containing TKA components, were
200 performed to examine the relationships between stiffness, mesh density,
201 and computation time.

202 **Figure 2** A plot showing the experimental force versus time plot (orange) in
203 comparison to the estimated forces (blue). Simulated forces were
204 estimated based upon the optimization results for stiffness and dissipation
205 constants. This plot represents only one trial. Plots for all trials can be
206 found in Appendix B.

207 **Figure 3** Component penetration (top row) and computation time (bottom row)
208 were more sensitive to material stiffness than the mesh density (# faces).
209 Low and stiffness constants resulted in excess penetration (negative
210 values) and increased computation time, respectively.

211
212

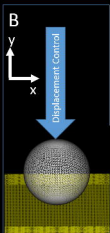
213

214 **References**

- 215 Cignoni, P., Callieri, M., Corsini, M., Dellepiane, M., Ganovelli, F., Ranzuglia, G., 2008.
216 MeshLab: an Open-Source Mesh Processing Tool, in: Scarano, V., Chiara, R.D.,
217 Erra, U. (Eds.), Eurographics Italian Chapter Conference. 129-136.
- 218 Delp, S.L., Anderson, F.C., Arnold, A.S., Loan, P., Habib, A., John, C.T., Guendelman,
219 E., Thelen, D.G., 2007. OpenSim: Open-Source Software to Create and Analyze
220 Dynamic Simulations of Movement. Biomedical Engineering, IEEE Transactions
221 54, 1940–1950.
- 222 Dunne, J., Ku, J., Seth, A., Delp, S.L., Hicks, J.L., Habib, A., Uchida, T., Pineda, B.,
223 2017a. OpenSim Forum: Elastic Foundation Model [WWW Document]. URL
224 [https://simtk.org/plugins/phpBB/viewtopicPhpbb.php?f=91&t=8380&p=22928&s](https://simtk.org/plugins/phpBB/viewtopicPhpbb.php?f=91&t=8380&p=22928&start=0&view=&sid=50dd5809b3bdb48c8c9525315c31eb30)
225 [tart=0&view=&sid=50dd5809b3bdb48c8c9525315c31eb30](https://simtk.org/plugins/phpBB/viewtopicPhpbb.php?f=91&t=8380&p=22928&start=0&view=&sid=50dd5809b3bdb48c8c9525315c31eb30)
- 226 Dunne, J., Ku, J., Seth, A., Delp, S.L., Hicks, J.L., Habib, A., Uchida, T., Pineda, B.,
227 2017b. OpenSim Forum: Penetrating Surfaces Between Triangular Meshes
228 [WWW Document]. URL
229 [https://simtk.org/plugins/phpBB/viewtopicPhpbb.php?f=91&t=8380&p=22928&s](https://simtk.org/plugins/phpBB/viewtopicPhpbb.php?f=91&t=8380&p=22928&start=0&view=&sid=50dd5809b3bdb48c8c9525315c31eb30)
230 [tart=0&view=&sid=50dd5809b3bdb48c8c9525315c31eb30](https://simtk.org/plugins/phpBB/viewtopicPhpbb.php?f=91&t=8380&p=22928&start=0&view=&sid=50dd5809b3bdb48c8c9525315c31eb30)
- 231 Dunne, J., Ku, J., Seth, A., Delp, S.L., Hicks, J.L., Habib, A., Uchida, T., Pineda, B.,
232 2013. OpenSim Forum: Trouble with Contact [WWW Document]. URL
233 [https://simtk.org/plugins/phpBB/viewtopicPhpbb.php?f=91&t=4404&p=16330&s](https://simtk.org/plugins/phpBB/viewtopicPhpbb.php?f=91&t=4404&p=16330&start=0&view=&sid=d8ccc62b05f6a94be41cf458211008fc)
234 [tart=0&view=&sid=d8ccc62b05f6a94be41cf458211008fc](https://simtk.org/plugins/phpBB/viewtopicPhpbb.php?f=91&t=4404&p=16330&start=0&view=&sid=d8ccc62b05f6a94be41cf458211008fc)

- 235 Fregly, B.J., Besier, T.F., Lloyd, D.G., Delp, S.L., Banks, S.A., Pandy, M.G., D’Lima,
236 D.D., 2012. Grand challenge competition to predict in vivo knee loads. *Journal of*
237 *Orthopaedic Research* 30, 503–513.
- 238 Hast, M.W., Piazza, S.J., 2013. Dual-joint modeling for estimation of total knee
239 replacement contact forces during locomotion. *Journal of Biomechanical*
240 *Engineering* 135, 021013.
- 241 Kim, H.J., Fernandez, J.W., Akbarshahi, M., Walter, J.P., Fregly, B.J., Pandy, M.G.,
242 2009. Evaluation of predicted knee-joint muscle forces during gait using an
243 instrumented knee implant. *Journal of Orthopaedic Research* 27, 1326–1331.
- 244 Kurtz, S., 2004. *The UHMWPE Handbook*, 1st ed. Academic Press, Philadelphia, PA, pp
245 319.
- 246 Kwon, O.-R., Kang, K.-T., Son, J., Kwon, S.-K., Jo, S.-B., Suh, D.-S., Choi, Y.-J., Kim,
247 H.-J., Koh, Y.-G., 2014. Biomechanical comparison of fixed- and mobile-bearing
248 for unicompartmental knee arthroplasty using finite element analysis. *Journal of*
249 *Orthopaedic Research* 32, 338–345.
- 250 Lenhart, R.L., Smith, C.R., Vignos, M.F., Kaiser, J., Heiderscheit, B.C., Thelen, D.G.,
251 2015. Influence of step rate and quadriceps load distribution on patellofemoral
252 cartilage contact pressures during running. *Journal of Biomechanics* 48, 2871–
253 2878.
- 254 Lin, Y.C., Fregly, B.J., 2010. Surrogate articular contact models for computationally
255 efficient multibody dynamic simulations. *Medical Engineering and Physics* 32,
256 584.

- 257 Muratoglu, O.K., Perinchief, R.S., Bragdon, C.R., O'Connor, D.O., Konrad, R., Harris,
258 W.H., 2003. Metrology to Quantify Wear and Creep of Polyethylene Tibial Knee
259 Inserts: Clinical Orthopaedics and Related Research 410, 155–164.
- 260 Schmitz, A., Piovesan, D., 2016. Development of an Open-Source, Discrete Element
261 Knee Model. IEEE Transactions of Biomedical Engineering 63, 2056–2067.
- 262 Shelburne, K.B., Torry, M.R., Pandy, M.G., 2006. Contributions of muscles, ligaments,
263 and the ground-reaction force to tibiofemoral joint loading during normal gait.
264 Journal of Orthopaedic Research 24, 1983–1990.
- 265 Sherman, M.A., Seth, A., Delp, S.L., 2011. Simbody: multibody dynamics for biomedical
266 research. Procedia IUTAM 2, 241–261.
- 267 Taylor, W.R., Heller, M.O., Bergmann, G., Duda, G.N., 2004. Tibio-femoral loading
268 during human gait and stair climbing. Journal of Orthopaedic Research 22, 625–
269 632.
- 270 Thompson, J.A., Hast, M.W., Granger, J.F., Piazza, S.J., Siston, R.A., 2011.
271 Biomechanical effects of total knee arthroplasty component malrotation: A
272 computational simulation. Journal of Orthopaedic Research 29, 969-75.
- 273 Uchida, T.K., Sherman, M.A., Delp, S.L., 2015. Making a meaningful impact: modelling
274 simultaneous frictional collisions in spatial multibody systems. Proceedings of
275 Math Physics and Engineering Science 471, 20140859.
- 276
- 277



Trial 10

